AIP | Review of Scientific Instruments

Temporally resolved plasma composition measurements by collective Thomson scattering in TEXTOR (invited)

M. Stejner, S. B. Korsholm, S. K. Nielsen, M. Salewski, H. Bindslev et al.

Citation: Rev. Sci. Instrum. **83**, 10E307 (2012); doi: 10.1063/1.4729503
View online: http://dx.doi.org/10.1063/1.4729503
View Table of Contents: http://rsi.aip.org/resource/1/RSINAK/v83/i10
Published by the American Institute of Physics.

Temporally resolved plasma composition measurements by collective Thomson scattering in TEXTOR (invited)[a)]

M. Stejner,[1,b)] S. B. Korsholm,[1] S. K. Nielsen,[1] M. Salewski,[1] H. Bindslev,[2] F. Leipold,[1] P. K. Michelsen,[1] F. Meo,[1] D. Moseev,[1,3] A. Bürger,[4] M. Kantor,[3,5] and M. de Baar[3]
[1]*Association EURATOM-DTU, Department of Physics, Technical University of Denmark, Risø Campus, DK-4000 Roskilde, Denmark*
[2]*Aarhus University, Faculty of Science and Technology, DK-8000 Aarhus C, Denmark*
[3]*FOM Institute DIFFER, Dutch Institute for Fundamental Energy Research, Association EURATOM-FOM, Trilateral Euregio Cluster, Nieuwegein, The Netherlands*
[4]*Association EURATOM-FZJ, D-52425 Jülich, Germany*
[5]*Ioffe Institute, RAS, Saint Petersburg 194021, Russia*

(Presented 9 May 2012; received 7 May 2012; accepted 24 May 2012; published online 25 June 2012)

Fusion plasma composition measurements by collective Thomson scattering (CTS) were demonstrated in recent proof-of-principle measurements in TEXTOR [S. B. Korsholm *et al.*, Phys. Rev. Lett. **106**, 165004 (2011)]. Such measurements rely on the ability to resolve and interpret ion cyclotron structure in CTS spectra. Here, we extend these techniques to enable temporally resolved plasma composition measurements by CTS in TEXTOR, and we discuss the prospect for such measurements with newly installed hardware upgrades for the CTS system on ASDEX Upgrade. [http://dx.doi.org/10.1063/1.4729503]

I. INTRODUCTION

At present there is no well-established method for measurements of the fuel ion ratio, n_T/n_D, in the core of a large, burning fusion plasma. With respect to ITER, it is unclear if the fuel ion ratio can be determined in the plasma core ($\rho < 0.3$) with the diagnostic set currently included in the ITER baseline design.[1] Such measurements would, however, be of importance for plasma control and machine protection, and a coordinated effort was recently undertaken to investigate new diagnostic concepts for fuel ion ratio measurements.[2] As part of this effort we have developed a new technique for plasma composition measurements by collective Thomson scattering (CTS). Here, we give an overview of this new diagnostic technique with particular emphasis on techniques for temporally resolved measurements of this type.

CTS diagnostics rely on measurements of electromagnetic probe radiation scattered off microscopic plasma fluctuations – principally in the electron density, but scattering from other types of fluctuations can also contribute.[3] The fluctuations relevant to CTS result mainly from electron screening of ions moving through the plasma. CTS can therefore provide access to information about confined ion populations. CTS has thus been applied in measurements of ion temperatures[4–7] and fast-ion velocity distributions[8–11] in fusion plasmas. The use of CTS for plasma composition measurements was demonstrated in recent proof-of-principle experiments at TEXTOR.[12,13] The technique developed for plasma composition measurements by CTS makes use of the combined spectral signatures of the ion cyclotron motion and of weakly damped ion Bernstein waves.[14] As illustrated in Figure 1, these create peaks in the CTS spectrum at regular intervals corresponding roughly to the cyclotron frequency of the dominant ion species in the plasma for scattering in a plane near perpendicular to the magnetic field. The peak heights, widths, and center frequencies are highly sensitive to the density and temperature of the thermal bulk ion populations. In particular, the relative size of peaks corresponding to different ion species is related to the relative densities of those ions. This so-called ion cyclotron structure therefore strongly enhances the sensitivity of CTS spectra to plasma composition. This sensitivity forms the basis for the proposed fuel ion ratio diagnostic. Measurements based on ion cyclotron structure in CTS spectra pose new challenges since peaks in the ion cyclotron structure are separated by only 20–40 MHz while standard CTS receiver setups used for fast-ion measurements typically provide a frequency resolution around 80–100 MHz. Resolving the ion cyclotron structure thus required development of new acquisition techniques for measurements with very high frequency resolution.[15] Below we shall introduce the techniques developed to meet these requirements and present the first temporally resolved plasma composition measurements based on ion cyclotron structure in CTS spectra.

II. MEASUREMENT TECHNIQUE

The probing radiation for the CTS system at TEXTOR (a/R = 0.46 m/1.76 m) is provided by a gyrotron operating at 110 GHz with an output power of 150 kW. As illustrated in Figure 2, the probing radiation is launched from the low-field side in the equatorial plane, and part of the scattered radiation is picked up by a receiving mirror located 20 cm above the entry of the probe beam. The measurement is localized in the scattering volume defined by the overlap of the probe

[a)]Invited paper, published as part of the Proceedings of the 19th Topical Conference on High-Temperature Plasma Diagnostics, Monterey, California, May 2012.
[b)]Author to whom correspondence should be addressed. Electronic mail: mspe@fysik.dtu.dk.

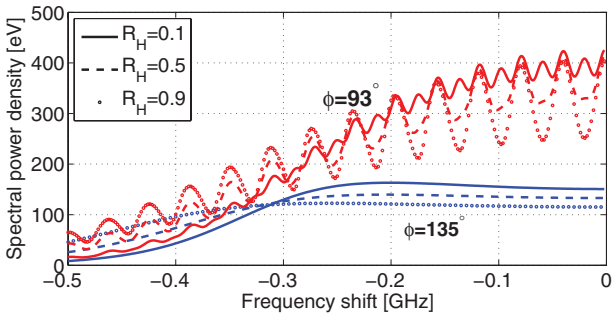

FIG. 1. Examples of CTS spectra simulated for conditions relevant to TEXTOR with different hydrogen isotope ratios, $R_H = n_H/(n_H + n_D)$, and different angles between the resolved fluctuation wave vector and the magnetic field, $\phi = \angle(\mathbf{k}^\delta, \mathbf{B})$. When ϕ is close to 90°, the spectra show ion cyclotron structure which is highly sensitive to plasma composition.

and receiver beams, and it resolves fluctuations in the plasma with wave vectors, $\mathbf{k}^\delta$, corresponding to the difference between the wave vectors of the received scattered and incident radiation, $\mathbf{k}^\delta = \mathbf{k}^s - \mathbf{k}^i$. The signal is sent through a quasi-optical transmission line to the receiver system located in the tokamak hall. The receiver is protected against stray radiation from the gyrotron by a pair of narrowband notch filters. The notch filters each attenuate the signal by 60 dB in a ~300 MHz wide frequency interval around the probe frequency. The gyrotron is generally operated in a pulsed mode in order to enable background subtraction.

Scattering from plasma fluctuations driven by thermal bulk ion populations introduces a frequency shift of a few hundred MHz, and peaks in the ion cyclotron structure are separated by 20–40 MHz. For measurements of the ion cyclotron structure, the receiver should therefore provide a frequency resolution around 1 MHz at frequencies around 109–111 GHz. The standard setup used for fast-ion measurements consists of a heterodyne receiver in which the signal is mixed down to the few GHz range and passed through a filterbank providing a frequency resolution of 80 MHz in the

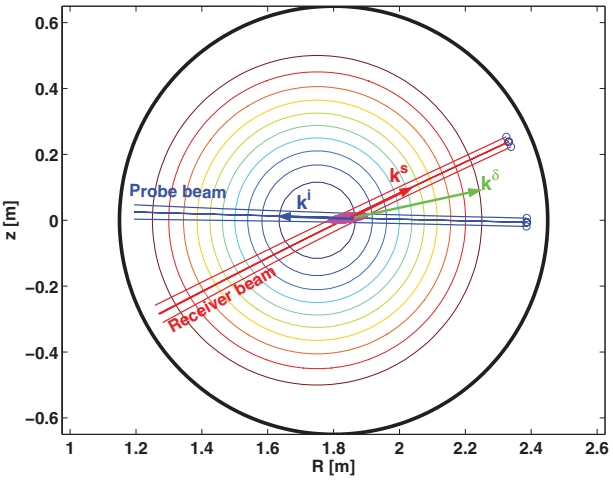

FIG. 2. A poloidal map illustrating the beam geometry used in TEXTOR for CTS measurements with $\phi = \angle(\mathbf{k}^\delta, \mathbf{B})$ close to 90°. Beam patterns representing the incident and received scattered radiation were calculated by ray tracing and are shown along with the relevant wave vectors (not to scale). The measurement is localized in the scattering volume at the intersection of the probe and receiver beams, and magnetic flux surfaces are indicated by circular contours.

109–111 GHz range. To achieve the resolution required for the present work, a second mixing stage was added and part of the spectrum in the range from 109.1 to 110.1 GHz was down-converted to a frequency range between 0.1 and 1.1 GHz. The down-converted signal was then passed to a Tektronix Digital Phosphor Oscilloscope (model DPO 7104) sampling the signal at 5×10^9 samples/s. The spectral power density was obtained by Fourier analysis using a sliding FFT window of 2^{13} samples. The downshifted part of the CTS spectrum was thus resolved with a frequency resolution of 0.6 MHz over the range of frequencies where the ion cyclotron structure is most significant. The spectra are subsequently binned and averaged in time to achieve a useful signal-to-noise ratio. The required integration time will be discussed below. A detailed description of this receiver setup, its sensitivity, and the initial data analysis has been given in Ref. 15. We also note that a similar technique has been used to study strong scattering phenomena in plasmas with tearing modes using the inline ECE receiver at TEXTOR.[16–19]

The acquisition technique described here easily meets the requirements on frequency resolution, but the high sample rate and limited memory on the oscilloscope constrains the total measurement time to 50 ms. Measurements over long time spans therefore requires careful management of the available memory. However, in initial experiments with this acquisition technique the overriding concern was not the temporal resolution. Rather, it was to obtain a signal-to-noise ratio sufficiently high to permit the ion cyclotron structure to be resolved. In addition, for these experiments acquisitions with the oscilloscope had to be triggered independently of the gyrotron cycle or events in the plasma. In these initial experiments, the gyrotron was therefore operated in a pulsed mode with 20 ms long on-periods separated by 5 ms off-periods, and the scattered signal from two on-periods was recorded with a single 50 ms long acquisition period. This provided both background measurements when the gyrotron was off and tens of milliseconds of integration time when the gyrotron was on – although parts of the on-periods were excluded due to strong drift in the gyrotron frequency after the gyrotron turn-on (the remaining drift is included in the data analysis and it is less severe when the gyrotron is operated at lower duty cycles[20]). This operating mode does achieve a very high signal-to-noise ratio, but it is not well suited for temporally resolved measurements.

To enable temporally resolved measurements over longer time spans, a method was developed to trigger short oscilloscope acquisition periods synchronized to individual gyrotron pulses. Each acquisition period thus contains a limited number of samples (up to the size of the memory) and is synchronized to the gyrotron modulation cycle. By delaying the acquisition relative to the trigger, it is further possible to exclude the time period right after the gyrotron turns on – thus avoiding the time when the gyrotron frequency drift is most significant. Based on experience from the initial proof-of-principle experiments, a signal-to-noise ratio of 10–20, sufficient to detect the ion cyclotron structure, can typically be achieved with an integration time less than 1 ms. For background subtraction, it is necessary to obtain measurements of both the CTS signal itself and of the background signal. We therefore adjust the delays and the lengths of the acquisition periods in order

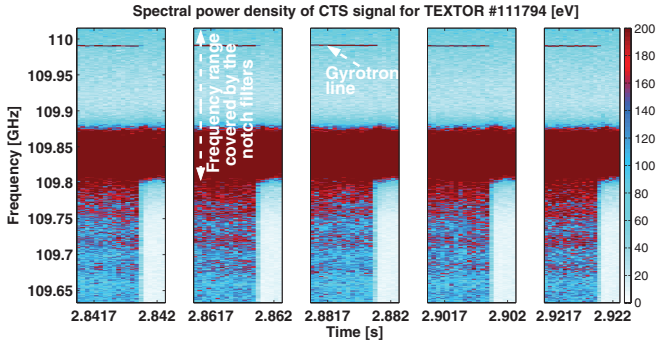

FIG. 3. Spectrogram showing the data recorded for 5 gyrotron pulses in TEXTOR discharge 111 794 before background subtraction and averaging over gyrotron on-periods. The data are binned in time with each bin corresponding to an average over 25 μs. Periods between gyrotron pulses, when no data were recorded, are skipped. The gyrotron line and the frequency interval covered by the notch filters are marked.

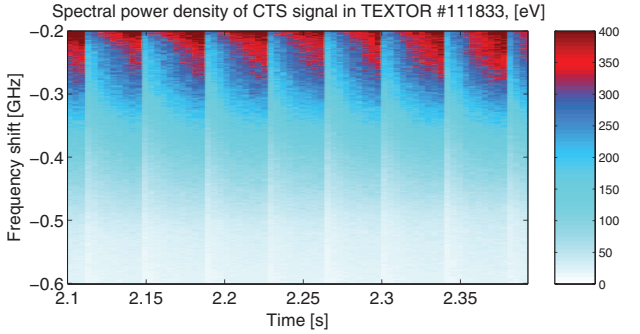

FIG. 4. A spectrogram showing data recorded in TEXTOR discharge 111 833 after background subtraction, adjustment for gyrotron frequency drift, and averaging over gyrotron on-periods. The gyrotron was modulated in a 2 ms on/2 ms off cycle which permits the strong sawtooth oscillations in this discharge to be resolved in time.

to measure across the gyrotron turn-off to provide coverage both when the gyrotron is on and when it is off.

For the present work, the gyrotron was modulated either in a 2 ms on/18 ms off cycle or, for discharge 111 833, in a 2 ms on/2 ms off cycle. Data were recorded with the oscilloscope in 0.5 ms long time windows for each gyrotron pulse. With the 2 ms on/18 ms off cycle, it was thus possible to cover 99 gyrotron pulses over a 2 s time interval. The acquisition windows covered 0.3 ms of gyrotron-on time and 0.1 ms of gyrotron-off time. Near the turn-off the gyrotron frequency can chirp strongly. Data in this interval, within 0.1 ms of the gyrotron turn-off, are excluded in subsequent analysis.

Figure 3 shows an example of a spectrogram recorded with this technique. The data are shown before background subtraction and averaging over gyrotron pulses. The CTS signal is generally two orders of magnitude larger than the background in the relevant frequency range, so the gyrotron-on periods can clearly be distinguished from the gyrotron-off periods. The gyrotron line can be seen at 109.99 GHz in the frequency range covered by the notch filters. Data in that frequency range cannot be accurately calibrated and are not useful except to monitor the gyrotron line. Data in the range covered by the notch filters are therefore excluded from further analysis. The gyrotron frequency drifts slightly for each cycle due to thermal expansion of the gyrotron cavity.[20] In subsequent analysis, this drift is taken into account by considering the spectral power density as a function of frequency shift relative to the gyrotron frequency. It may also be noted that gyrotron on/off times can be clearly identified by monitoring the amplitude of the gyrotron line. In Figure 3, the data are binned in time, so each pixel along the abscissa corresponds to an average over 25 μs allowing the different phases in each acquisition period to be resolved. In subsequent analysis, the background measured when the gyrotron is off is subtracted, and data from the gyrotron on-periods are averaged to obtain one spectrum for each gyrotron pulse.

Figures 4–6 show examples of data from TEXTOR analyzed with this procedure. Figure 4 shows data from discharge 111 833 which was designed for sawteeth oscillations with relatively long periods (~40 ms). With the rapid gyrotron modulation, the sawtooth cycle can be resolved in time, and the sawteeth are clearly seen in the CTS signal due to their effects on the plasma density and temperature – a detailed discussion of the effects of sawteeth on CTS signal was given in Ref. 9. Similar, though typically smaller, fluctuations can be found in data from other discharges discussed here. Figure 5 shows an example of data taken during a so-called overlap sweep in discharge 111 831: to determine the optimal mirror position, the receiver mirror was moved to sweep the receiver beam across the probe beam. As an overlap between the two beams is gradually established, the CTS signal grows in intensity and then decays as the overlap disappears. This behavior corresponds closely to that of the CTS signal in the filterbank channels of the standard CTS receiver setup used for fast-ion measurements. Figure 5 shows a comparison of the signal in these channels and the signal seen with the oscilloscope in the corresponding frequency bands. Though the two are generally consistent, differences between the absolute signal levels for some channels could indicate small inaccuracies in the calibration of either of the two systems (which are independently calibrated by different methods).

The ability to resolve such effects demonstrates that the oscilloscope can be used for measurements over long time spans by economizing the available memory. However, in discharges 111 831 and 111 833, the angle between the resolved

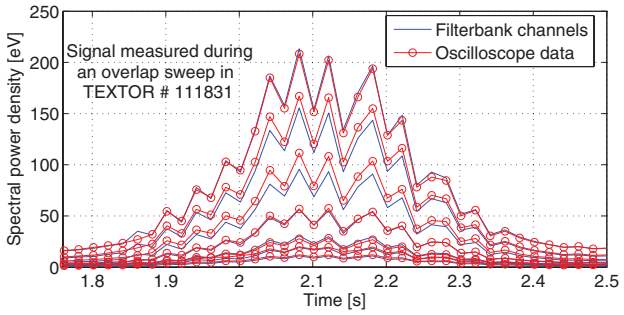

FIG. 5. A comparison between the signal seen during an overlap sweep in discharge 111 831 with some of the filterbank channels of the standards CTS receiver setup (channels 13-19, covering the range from 109.27 to 109.75 GHz) and the average spectral power density measured by the oscilloscope in the corresponding frequency bands. The intensity and time dependence of the two signals correspond well to each other showing that the calibration of the two systems are consistent and that the oscilloscope can be used for measurements over long time spans.

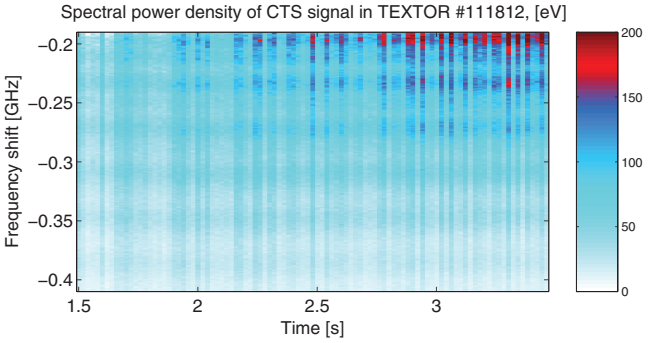

FIG. 6. The CTS spectral power density measured during a density scan in discharge 111 812. The ion cyclotron structure can be seen as horizontal bands of elevated signal intensity. The spectral power density grows and the ion cyclotron structure becomes more prominent as the density increases with time.

fluctuation wave vector and the magnetic field was ∼20° from perpendicular, $\phi \cong 110°$. For this geometry, the CTS spectrum does not show any ion cyclotron structure. By contrast the resolved angle in discharge 111 794 was close enough to perpendicular, $\phi \cong 93°$, for the spectrum to contain ion cyclotron structure. This may be seen in the spectrogram in Figure 3 as bands of elevated intensity at frequencies outside the notch filters. Figure 6 gives an example of data measured for $\varphi \cong 93°$ in a time interval with varying plasma parameters. A density sweep was conducted in this discharge, 111 812, and within the CTS measurement interval the central electron density increased from 3.5 to 5.5 × 10^{19} m^{-3}. As expected from theory, the spectral power density in the CTS spectrum increases and the ion cyclotron structure becomes more prominent during the density sweep – see also Figure 7 for examples of individual spectra. Thus, the techniques described here enable measurements over timescales sufficiently long for significant changes in plasma conditions to take place, and effects of such changes can be detected in the measured spectra.

III. ANALYSIS OF MEASURED SPECTRA

For quantitative interpretation, we fit the measured spectra with a theoretical model for CTS[3,21] using a Bayesian least-squares method of inference[22] frequently employed in analysis of CTS data from TEXTOR. The model assumes a homogeneous plasma in the scattering volume, treats the

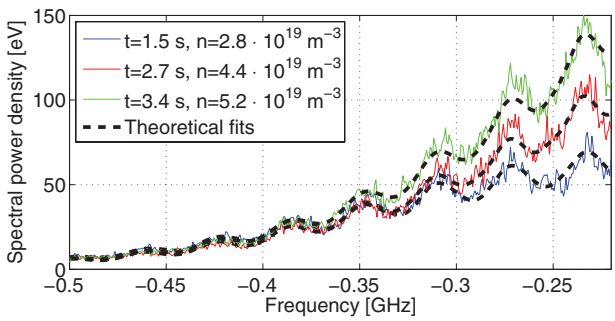

FIG. 7. Examples of fits to CTS spectra measured in discharge 111 812. From below, the spectra are plotted in order of increasing time and density. The fits reproduce the spectra with reasonable accuracy considering the uncertainties involved. Residuals are within or close to the noise level estimated as the standard error of the mean spectrum within each gyrotron pulse.

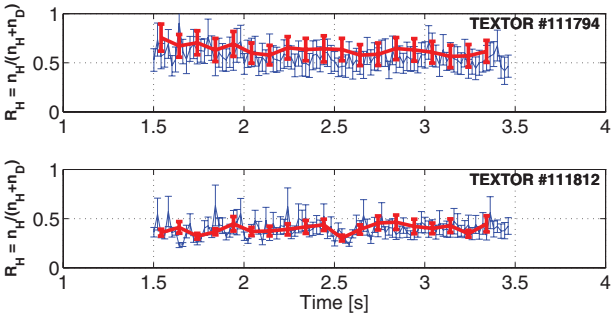

FIG. 8. Hydrogen isotope ratios, $R_H = n_H/(n_H + n_D)$, inferred from the CTS measurements in discharges 111 794 (upper panel) and 111 812 (lower panel). The thin lines show results of fits to spectra measured in individual gyrotron pulses. The thick lines represent results of fits to spectra obtained by averaging over 5 gyrotron pulses. The error bars represent intervals of two standard deviations of the posterior probability distribution for R_H.

scattering process in a fully electromagnetic approach, and describes the plasma fluctuations which cause the scattering within a kinetic theory. The Bayesian approach permits prior knowledge about all model parameters as well as uncertainties in both the prior knowledge and in the measured CTS spectra to be incorporated in the analysis. A detailed description of the analysis of CTS spectra with ion cyclotron structure within this method was given for the first such measurements on TEXTOR,[13] and here we follow the approach developed in that work.

Figure 7 shows examples of measured and fitted spectra from discharge 111 812. The fits reproduce the measured spectra with residuals within or close to the noise level in the measurements (i.e., within one standard deviation of temporal fluctuations in the mean CTS signal for each gyrotron pulse). Figure 8 shows the hydrogen isotope ratio, $R_H = n_H/(n_H + n_D)$, inferred from fits to the CTS spectra measured in discharges 111 794 and 111 812. Discharge 111 794 was fuelled with hydrogen through neutral beam injection (P_{NBI} = 1.26 MW) and with deuterium through gas puffing during the discharge. Here, the CTS results indicate a composition dominated by hydrogen-with R_H decreasing slightly from values around 0.7 to values around 0.6 during the measurement interval. Discharge 111 812 was fuelled only with deuterium through gas puffing, but wall recycled hydrogen may be expected to contribute to the composition. In this discharge, the results indicate a lower hydrogen concentration, $R_H \cong 0.4$, and no appreciable change in composition is detected during the density scan.

Within the Bayesian least-squares method of inference used here, the uncertainties of the inferred values of R_H can be estimated theoretically[22,23] from the width of the posterior probability distribution for R_H. Such estimates are shown in Figure 8 as error bars representing plus/minus one standard deviation of the posterior probability distribution function. In a plasma composed of hydrogen and deuterium, scattering off fluctuations driven by the motion of hydrogen tend to dominate the CTS signal unless R_H is small.[14] For such plasmas, CTS spectra are therefore more sensitive to the composition at lower values of R_H. So the statistical uncertainties for R_H are smaller in discharge 111 812 than in discharge 111 794. However, we note that a similar mechanism does not apply to

measurements in plasmas composed of deuterium and tritium. These isotopes have a more similar charge-to-mass ratio, and for equal densities their contributions to the CTS spectrum are similar in magnitude.[14] On ITER the greatest sensitivity to plasma composition would therefore be attained for n_T/n_D just below one.[23]

Uncertainties in the present measurements can be reduced by combining measurements from several gyrotron pulses and fitting the average spectrum. The thick red lines in Figure 8 give results of fits to spectra resulting from an average over 5 gyrotron pulses each (i.e., corresponding to 1.5 ms of gyrotron-on time each). The results are consistent with the fits to data from individual gyrotron pulses (thin lines), and fluctuations as well as statistical uncertainties in the inferred values of R_H are smaller due to the higher signal-to-noise ratio in the fitted spectra. However, the temporal resolution is also reduced, and sufficiently rapid changes in plasma conditions could in principle distort the spectra if conditions change significantly during the period averaged over. Alternatively, in future experiments, the integration times for each gyrotron pulse could be lengthened. However, depending on the required sample rate and the available memory, this would reduce the number of gyrotron pulses that can be covered. As will be discussed below, a system addressing some of these challenges is being installed on ASDEX Upgrade.

IV. PROSPECTS FOR PLASMA COMPOSITION MEASUREMENTS BY CTS ON ASDEX UPGRADE

A CTS system has been installed on ASDEX Upgrade[24,25] and used for measurements of the fast-ion velocity distribution.[10] As with the TEXTOR system, the probing radiation is provided by a gyrotron (here at 105 GHz), and the CTS signal is usually resolved by means of a heterodyne receiver with a filterbank providing a frequency resolution of 100 MHz in the range from 103 to 107 GHz.[26] This system has been modified to enable measurements with high frequency resolution through direct digitization and Fourier analysis of the CTS signal. While the details are different, the principles of the modified setup is similar to that used on TEXTOR.[15] The CTS signal is split with a power divider, and by means of two heterodyne mixing stages one part of the CTS signal is measured with the filterbank while another part in the range from 104 to 106.6 GHz is down-converted to the range between 0.4 and 3 GHz with the probing frequency down-converted to 1.4 GHz. The down-converted signal is then measured by a fast digitizer, the NI PXIe-5186. This 8-bit digitizer has an analogue bandwidth of 5 GHz, 1 GB memory and can sample the signal at rates up to 12.5×10^9 samples/s. This setup will permit a broader part of the CTS spectrum to be digitized over longer time intervals than were possible with the TEXTOR system. In addition, a new trigger system has been developed providing greater flexibility in the operation of both the gyrotron and the CTS receiver, which can be triggered independently of each other at any time during a discharge. The modified system is currently being commissioned, and results of this work will be reported elsewhere. Here, we discuss the requirements on integration time and the limitations this places on the temporal resolution.

ASDEX Upgrade is usually operated with deuterium dominated plasmas, but operation with minority hydrogen and helium populations is also possible. Part of the goals for the modified CTS system is to investigate the effects of helium on CTS spectra and the feasibility of measuring the density of thermal helium in fusion plasmas by CTS. We therefore wish to estimate the integration time required to achieve a reasonable accuracy of the inferred plasma composition, which is here parameterized either by R_H for plasmas composed of hydrogen and deuterium or by $R_{He} = n_{He}/(n_{He}+n_D)$ for plasmas composed of helium and deuterium.

Within the method of inference described above, the theoretically expected accuracy of CTS measurements can be estimated for a given plasma scenario on the basis of assumptions about the expected signal-to-noise ratio of the CTS spectrum and the accuracy of prior knowledge about model parameters.[22,23] On TEXTOR, the signal-to-noise ratio in the oscilloscope measurements corresponds well to theoretical expectations for noise in CTS measurements when accounting for the effects of background subtraction:[27] $\mathrm{SNR} = P_s(WT)^{1/2}/(2(P_s + P_b)^2 + 2P_b^2)^{1/2}$, where P_s is the spectral power density of the CTS spectrum, P_b is the spectral power density of the background signal, W is the frequency resolution, and T is the integration time, half of which is assumed to be used for background measurements. On ASDEX Upgrade, the background is higher than on TEXTOR, ~50 eV instead of 10 eV. However, the output power of the gyrotron is also higher, 600 kW instead of 150 kW, so the spectral power density of the CTS signal is higher, and the achievable signal-to-noise ratio is not expected to change significantly. On the other hand, the temperatures and densities of plasmas in ASDEX Upgrade are higher which can affect the sensitivity of the CTS spectrum. Here, we assume parameters relevant for a neutral beam heated H-mode plasma, $n_e = 6 \times 10^{19}$ m^{-3}, $T_e = T_i = 2.5$ keV, and we assume a scattering geometry with $\varphi = 93^\circ$. We further assume that the temperature and density are known with uncertainties of 10% and that the angles characterizing the scattering geometry are known within 2°.

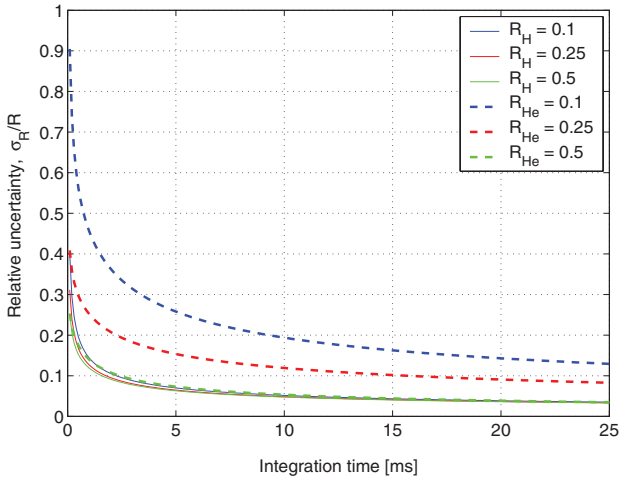

FIG. 9. The theoretically expected relative uncertainty for CTS measurements of R_H in hydrogen/deuterium dominated plasmas (thin lines) and of R_{He} in helium/deuterium dominated plasmas (thick dashed lines) on ASDEX Upgrade. Results for σ_{RH}/R_H depend little on R_H itself and are nearly coincident with results for σ_{RHe}/R_{He} with $R_{He} = 0.5$.

Figure 9 shows the theoretically expected relative uncertainties for R_H and R_{He} based on these assumptions for a range of plasma compositions and integration times. In a plasma consisting of hydrogen and deuterium, the relative uncertainty, σ_{RH}/R_H, is nearly constant as a function of R_H, and uncertainties below 20% can be achieved for integration times longer than 1.5 ms. In plasmas consisting of helium and deuterium, the required integration times are longer and depend strongly on R_{He}. Integration times above 10 ms are required to reach uncertainties below 20% for $R_{He} = 0.1$ (i.e., for $\sigma_{RHe} < 0.02$ in absolute terms). Assuming a sample rate of 6.25 GHz, the digitizer can measure the CTS signal for a total of 160 ms. Thus, the system is capable of 106 measurements of R_H in hydrogen/deuterium plasmas or 16 measurements of R_{He} in deuterium dominated helium/deuterium plasmas. Especially in the latter case, acquisitions periods should thus be carefully timed relative to expected changes in the plasma composition.

V. CONCLUSION

The first proof-of-principle plasma composition measurements by CTS on TEXTOR demonstrated the ability to resolve and interpret ion cyclotron structure in CTS spectra.[12,13] Here, we have discussed new techniques enabling temporally resolved plasma composition measurements, and we have shown the first measurements of plasma composition dynamics by CTS. This expands the range and applicability of measurements based on ion cyclotron structures in CTS spectra. Apart from measurements of dynamics in the plasma core, it is worth noting that this enables studies of the plasma composition profile, which can be obtained by gradually moving the CTS scattering volume across the plasma to obtain measurements at different positions within a single discharge. Analysis of such experiments is in progress and will be reported elsewhere. While all data analysis is presently done off-line after the measurements, it should also be noted that techniques for real-time Fourier analysis are under development for related diagnostics,[19] which in the long run may also help enable real-time plasma composition measurements by CTS.

Plasma composition measurements by CTS are of particular interest with respect to the potential use of CTS as a fuel ion ratio diagnostic in future experiments with burning fusion plasmas. While the detailed requirements to implement a CTS fuel ion ratio diagnostic on ITER have not been studied, it is reasonable to expect that such a system could be conceptually very similar to the CTS system proposed for fast-ion measurements on ITER.[28,29] Thus, preliminary studies indicate that the quasi-optical components for a CTS fuel ion ratio diagnostic could be integrated in a fast-ion system,[30,31] and sensitivity studies indicate that such a system could in principle fulfill the ITER measurement requirements for fuel ion ratio diagnostics.[23]

At present, work is underway to enable plasma composition measurements by CTS on ASDEX Upgrade. We here discussed the prospect for temporally resolved measurements with this system. Our results indicate that the new receiver setup should be capable of up to 106 measurements with 1.5 ms time resolution of R_H in hydrogen/deuterium plasmas, or up to 16 measurements with 10 ms time resolution of R_{He} in deuterium dominated helium/deuterium plasmas. The memory size of the data acquisition card is a limiting factor in this respect, and options to stream the data from the memory to permanent storage during the discharge are being studied in order to overcome some of these restrictions.

ACKNOWLEDGMENTS

The authors wish to acknowledge essential cooperation with the TEXTOR team and to thank them for helpful support throughout this work. This work has been supported by the European Communities under the contract of Association between EURATOM and the Technical University of Denmark. It was carried out within the framework of the European Fusion Development Agreement under EFDA Contract No. WP10-DIA-01-03 fuel ion ratio. The views and opinions expressed herein do not necessarily reflect those of the European Commission.

[1] A. J. H. Donné *et al.*, Nucl. Fusion **47**, S337 (2007).
[2] S. B. Korsholm *et al.*, Rev. Sci. Instrum. **81**, 10D323 (2010).
[3] H. Bindslev, J. Atmos. Terr. Phys. **58**, 983 (1996).
[4] G. Wurden, M. Ono, and K. Wong, Phys. Rev. A **26**, 2297 (1982).
[5] H. Park, P. S. Lee, W. A. Peebles, and N. C. Luhmann, Rev. Sci. Instrum. **56**, 922 (1985).
[6] R. Behn, D. Dicken, J. Hackmann, S. Salito, M. Siegrist, P. Krug, I. Kjelberg, B. Duval, B. Joye, and A. Pochelon, Phys. Rev. Lett. **62**, 2833 (1989).
[7] E. V. Suvorov *et al.*, Plasma Phys. Controlled Fusion **37**, 1207 (1995).
[8] H. Bindslev *et al.*, Phys. Rev. Lett. **97**, 205005 (2006).
[9] S. K. Nielsen *et al.*, Nucl. Fusion **51**, 063014 (2011).
[10] M. Salewski *et al.*, Nucl. Fusion **50**, 035012 (2010).
[11] D. Moseev *et al.*, Plasma Phys. Controlled Fusion **53**, 105004 (2011).
[12] S. B. Korsholm *et al.*, Phys. Rev. Lett. **106**, 165004 (2011).
[13] M. Stejner *et al.*, Plasma Phys. Controlled Fusion **54**, 015008 (2012).
[14] M. Stejner, S. K. Nielsen, H. Bindslev, S. B. Korsholm, and M. Salewski, Plasma Phys. Controlled Fusion **53**, 065020 (2011).
[15] M. Stejner *et al.*, Rev. Sci. Instrum. **81**, 10D515 (2010).
[16] J. W. Oosterbeek *et al.*, Rev. Sci. Instrum. **79**, 093503 (2008).
[17] D. J. Thoen *et al.*, Rev. Sci. Instrum. **80**, 103504 (2009).
[18] E. Westerhof *et al.*, Phys. Rev. Lett. **103**, 125001 (2009).
[19] W. A. Bongers *et al.*, Rev. Sci. Instrum. **82**, 063508 (2011).
[20] P. Woskov *et al.*, Rev. Sci. Instrum. **77**, 10E524 (2006).
[21] H. Bindslev, Plasma Phys. Controlled Fusion **35**, 1615 (1993).
[22] H. Bindslev, Rev. Sci. Instrum. **70**, 1093 (1999).
[23] M. Stejner, S. B. Korsholm, S. K. Nielsen, M. Salewski, H. Bindslev, V. Furtula, F. Leipold, P. K. Michelsen, F. Meo, and D. Moseev, Nucl. Fusion **52**, 023011 (2012).
[24] F. Meo *et al.*, Rev. Sci. Instrum. **79**, 10E501 (2008).
[25] F. Meo *et al.*, J. Phys.: Conf. Ser. **227**, 012010 (2010).
[26] V. Furtula, M. Salewski, F. Leipold, P. K. Michelsen, S. B. Korsholm, F. Meo, D. Moseev, S. K. Nielsen, M. Stejner, and T. Johansen, Rev. Sci. Instrum. **83**, 013507 (2012).
[27] H. Bindslev, "On the theory of Thomson scattering and reflectometry in a relativistic magnetized plasma," Ph.D. dissertation, Risø National Laboratory, Roskilde, Denmark, 1992.
[28] H. Bindslev, F. Meo, and S. B. Korsholm, *ITER Fast Ion Collective Thomson Scattering - Feasibility Study* (2003), see http://www.risoecampus.dtu.dk/DTU_Fysik/Projects_Fusion_Plasma/fusion_CTS/ITER.aspx.
[29] H. Bindslev, A. W. Larsen, F. Meo, P. Michelsen, S. Michelsen, A. H. Nielsen, S. Nimb, and E. Tsakadze, ""ITER fast ion collective Thomson scattering," Final Report, EFDA Contract 04-1213 - Deliverable 4.1-D3, 2005, see http://www.risoecampus.dtu.dk/DTU_Fysik/Projects_Fusion_Plasma/fusion_CTS/ITER.aspx.
[30] F. Meo, H. Bindslev, and S. B. Korsholm, *ITER Fast Ion Collective Thomson Scattering, Conceptual Design of 60 GHz System* (2007), see http://www.risoecampus.dtu.dk/DTU_Fysik/Projects_Fusion_Plasma/fusion_CTS/ITER.aspx.
[31] F. Meo, H. Bindslev, S. B. Korsholm, E. L. Tsakadze, C. I. Walker, P. Woskov, and G. Vayakis, Rev. Sci. Instrum. **75**, 3585 (2004).